

## Oligonucleotide#Oligospermine Conjugates (Zip Nucleic Acids): A Convenient Means of Finely Tuning Hybridization Temperatures

Re#gis Noir, Mitsuharu Kotera, Be#ne#dicte Pons, Jean-Serge Remy, and Jean-Paul Behr

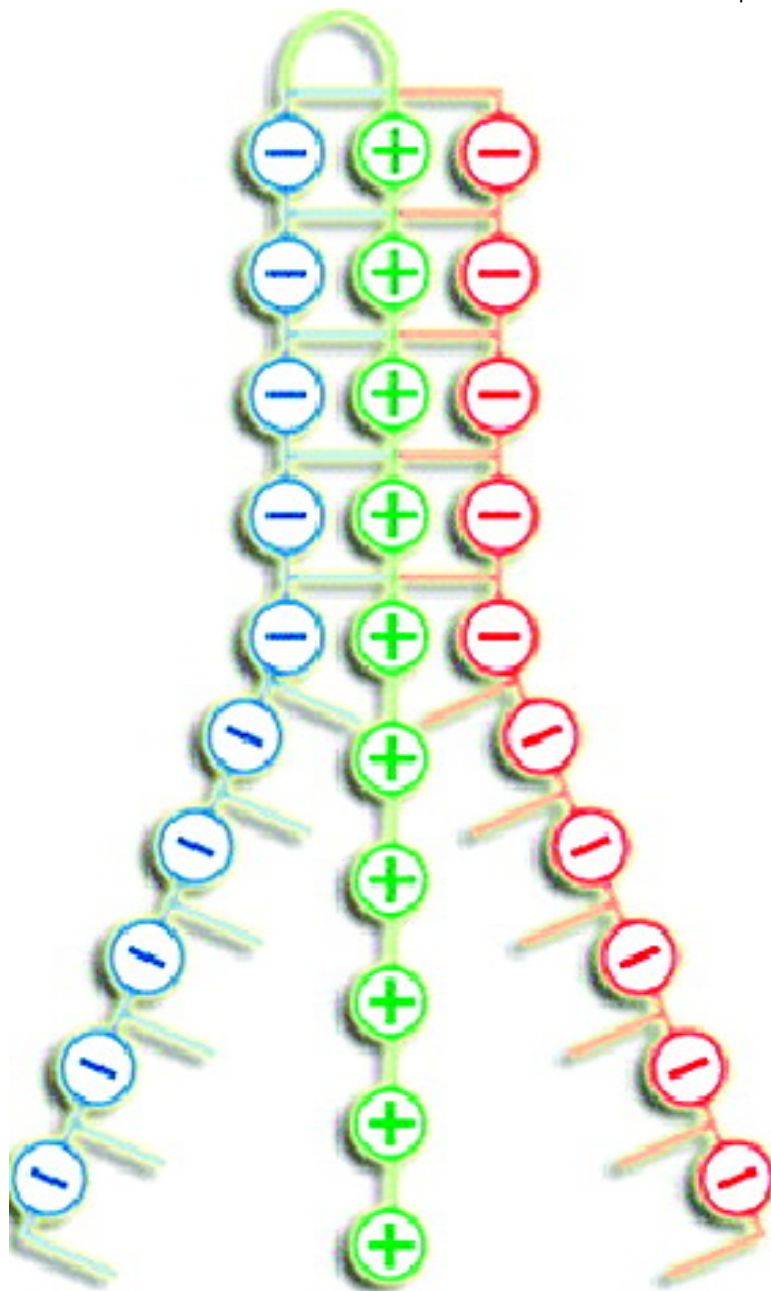
*J. Am. Chem. Soc.*, **2008**, 130 (40), 13500-13505 • DOI: 10.1021/ja804727a • Publication Date (Web): 10 September 2008

Downloaded from <http://pubs.acs.org> on December 15, 2008



ACS Publications  
High quality. High impact.

Journal of the American Chemical Society is published by the American Chemical Society, 1155 Sixteenth Street N.W., Washington, DC 20036



### More About This Article

---

Additional resources and features associated with this article are available within the HTML version:

---

- Supporting Information
- Access to high resolution figures
- Links to articles and content related to this article
- Copyright permission to reproduce figures and/or text from this article

[View the Full Text HTML](#)



## Oligonucleotide–Oligospermine Conjugates (Zip Nucleic Acids): A Convenient Means of Finely Tuning Hybridization Temperatures

Régis Noir, Mitsuharu Kotera, Bénédicte Pons, Jean-Serge Remy, and Jean-Paul Behr\*

*Laboratoire de Chimie Génétique associé CNRS et Université de Strasbourg, Faculté de Pharmacie, 67401 Illkirch, France*

Received June 20, 2008; E-mail: behr@pharma.u-strasbg.fr

**Abstract:** Synthesis of oligonucleotide probes and control of their hybridization temperature are key aspects of polymerase chain reaction (PCR)-based detection of genetic sequences. A straightforward means to approach the last goal is to decrease the repulsion between the polyanionic probe and target strands. To this end, we have developed a versatile automated synthesis of oligonucleotide–oligospermine derivatives that gave fast access to a large variety of compounds. Plots of their hybridization temperatures  $T_m$  vs overall charge provided a measure of the impact of interstrand phosphate repulsion (and of spermine-mediated attraction) on the main driving force of duplex formation, i.e., base pairing. It showed that stabilization brought about by excess cationic charges can be of larger absolute magnitude than interstrand repulsion, even in high salt media. Base sequence and conjugation site (3' or 5') hardly influenced the effect of spermine on  $T_m$ . In typical PCR probe conditions, the  $T_m$  increased linearly with the number of grafted spermines (e.g., 6.2 °C per spermine for a decanucleotide probe). The large data set of  $T_m$  vs number of spermines and oligonucleotide length allowed us to empirically derive a simple mathematical relation that is accurately predicting the  $T_m$  of any oligonucleotide–oligospermine derivative. Zip nucleic acids (ZNA) are thus providing an interesting alternative to locked nucleic acids (LNA) or minor groove binders (MGB) for raising the stability of 8–12-mer oligonucleotides up to ca. 70 °C, the level required for quantitative PCR experiments.

### Introduction

Molecular biology and diagnostic techniques using genomic information rely on sequence recognition by oligonucleotide probes. Their sustained development and widespread use is mobilizing chemist's imagination since discovery of the polymerase chain reaction (PCR). Among fruitful ideas, target sequence detection with molecular beacons,<sup>1</sup> and enhanced hybridization using MGB<sup>2</sup> or LNA<sup>3</sup> probes have been translated into numerous reagents and diagnostic kits, but time saving is pushing the boundaries of diagnosis techniques still further. For example, simultaneous detection of three antibiotic-resistant bacteria strains in a patient sample by multiplex real-time PCR would require a mixture of up to nine oligonucleotides. In such complex cases, chemical modification can help to raise each oligonucleotide hybridization temperature to the desired temperature as dictated by the experiment or eventually allow detection of several sequences with the same fluorophore by shifting their characteristic melting to different temperatures. Yet in practice, the synthesis of the modified oligonucleotides

must remain simple and inexpensive and the increase of hybridization temperature should be tunable and predictable.

In this context, overcoming the electrostatic repulsion between anionic nucleic acid strands appears as a straightforward general means of improving hybridization. Among the many approaches developed over 2 decades,<sup>4–15</sup> only those not inhibiting the nucleic acid-processing enzymes are

- (1) Piatek, A. S.; Tyagi, S.; Pol, A. C.; Telenti, A.; Miller, L. P.; Kramer, F. R.; Alland, D. *Nat. Biotechnol.* **1998**, *16*, 359–363.
- (2) Kutyavin, I. V.; Afonina, I. A.; Mills, A.; Gorn, V. V.; Lukhtanov, E. A.; Belousov, E. S.; Singer, M. J.; Walburger, D. K.; Lohkov, S. G.; Gall, A. A.; Dempcy, R.; Reed, M. W.; Meyer, R. B.; Hedgpeth, J. *Nucleic Acids Res.* **2000**, *28*, 655–661.
- (3) Koshkin, A. A.; Nielsen, P.; Meldgaard, M.; Rajwanshi, V. K.; Singh, S. K.; Wengel, J. *J. Am. Chem. Soc.* **1998**, *120*, 13252–13253.

- (4) Lemaitre, M.; Bayard, B.; Lebleu, B. *Proc. Natl. Acad. Sci. U.S.A.* **1987**, *84*, 648.
- (5) Zhu, T.; Wei, Z.; Tung, C. H.; Dickerhof, W. A.; Breslauer, K. J.; Georgopoulos, D. E.; Leibowitz, M. J.; Stein, S. *Antisense Res. Dev.* **1993**, *3*, 265–275.
- (6) Barawkar, D. A.; Kumar, V. A.; Ganesh, K. N. *Biochem. Biophys. Res. Commun.* **1994**, *205*, 1665–1670.
- (7) Schmid, N.; Behr, J.-P. *Tetrahedron Lett.* **1995**, *36*, 1447–1450.
- (8) Corey, D. R. *J. Am. Chem. Soc.* **1995**, *117*, 9373–9374.
- (9) Manoharan, M.; Ramasamy, K. S.; Mohan, V.; Cook, P. D. *Tetrahedron Lett.* **1996**, *37*, 7675–7678.
- (10) Chaturvedi, S.; Horn, T.; Letsinger, R. L. *Nucleic Acids Res.* **1996**, *24*, 2318–2323.
- (11) Barawkar, D. A.; Bruce, T. C. *Proc. Natl. Acad. Sci. U.S.A.* **1998**, *95*, 11047–11052.
- (12) Harrison, J. G.; Balasubramanian, S. *Nucleic Acids Res.* **1998**, *26*, 3136–3145.
- (13) Astriab-Fisher, A.; Sergueev, D.; Fisher, M.; Shaw, B. R.; Juliano, R. L. *Pharm. Res.* **2002**, *19*, 744–754.
- (14) Michel, T.; Martinand-Mari, C.; Debart, F.; Lebleu, B.; Robbins, I.; Vasseur, J. *J. Nucleic Acids Res.* **2003**, *31*, 5282–5290.
- (15) Stetsenko, D. A.; Williams, D.; Gait, M. J. *Nucleic Acids Res. Suppl.* **2001**, 153–154.
- (16) Venkatesan, N.; Kim, B. H. *Chem. Rev.* **2006**, *106*, 3712–3761.

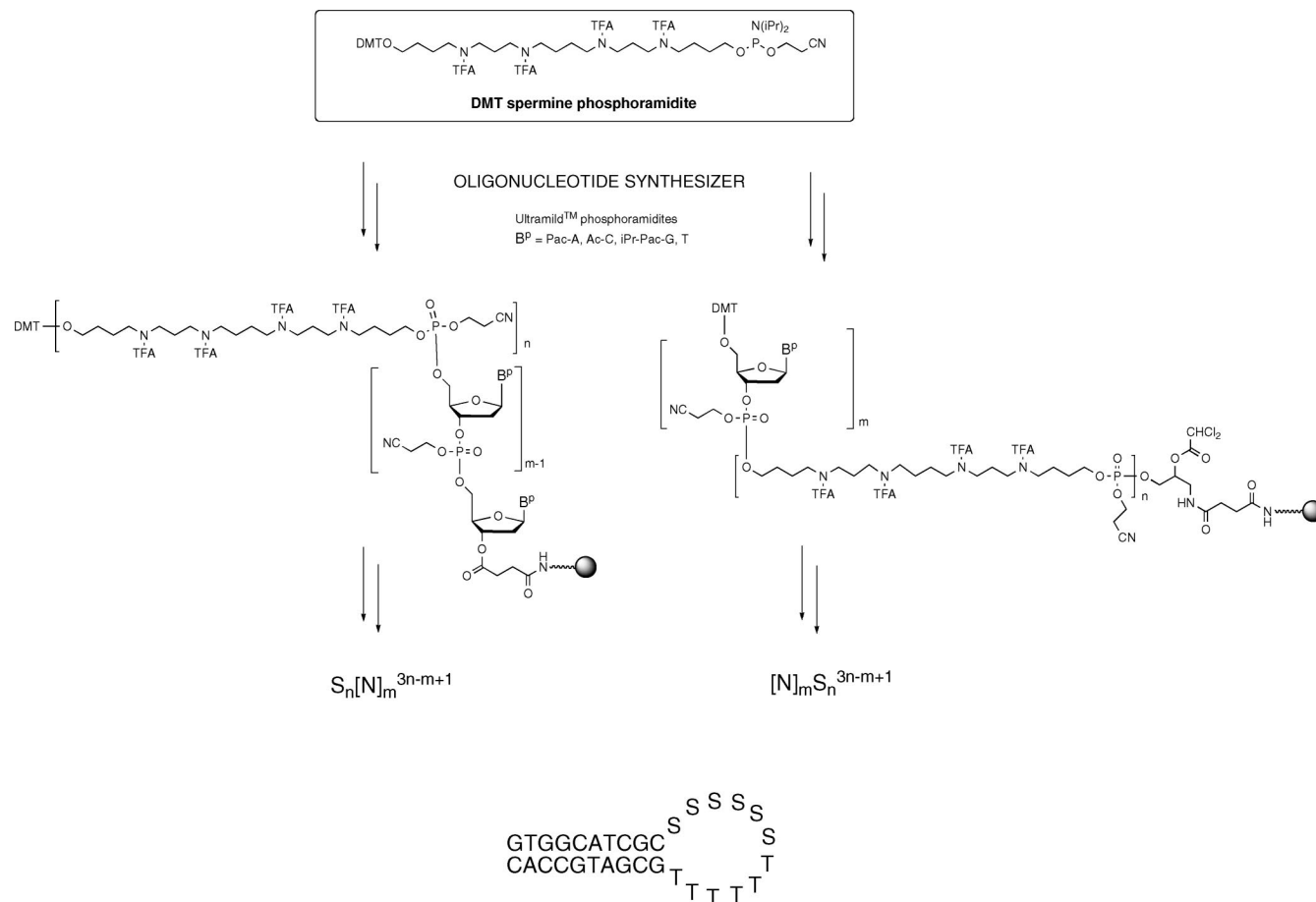


**Figure 1.** Solid-phase synthesis of oligonucleotide–oligospermine derivatives using the phosphoramidite coupling chemistry. Spermine can be introduced at the 5′-end (left), at the 3′-end (right), or within the oligonucleotide sequence (hairpin loop).

of interest here. Oligonucleotide–cationic peptide conjugates (for a review, see 16) would satisfy this condition as well as the aforementioned practical limitations. However, stepwise automated synthesis of oligonucleotide–oligopeptides requires compatible phosphodiester- and amide-forming chemistries and is still in progress. We recently described another automated solid-phase synthesis of cationic oligonucleotide conjugates<sup>17</sup> that is entirely based on the phosphoramidite coupling chemistry used for the synthesis of oligonucleotides. This approach is using a fully trifluoroacetyl-protected dimethoxytritylspermine phosphoramidite derivative which is compatible with oligonucleotide synthesis. Coupling yields have been optimized, and the versatility of this approach is demonstrated here with the synthesis of various oligonucleotide sequences and length and sequential addition of up to 20 spermine residues. Analysis of the large set of measured melting temperatures allowed us to extract the electrostatic contribution to duplex stability and derive a simple relation for predicting the stability increase brought about by a grafted spermine residue on any oligonucleotide. As a consequence of the intrinsic difficulties of conjugating oligonucleotides to oligocations,<sup>18</sup> the only other systematic analysis published to date was performed with octanucleotide–peptide conjugates bearing up to five cationic amino acid residues.<sup>12</sup>

## Results and Discussion

In addition to their synthesis, the main goal of this work was to circumvent the structural factors governing hybridization of cationic oligonucleotides to complementary oligonucleotides and complementary cationic oligonucleotides by studying the effect of the charges and 3′/5′ location of the cationic moiety on stability. Melting temperatures were measured in physiological ionic strength (150 mM sodium chloride) and pH 7.4, with complementary sequences of identical length forming a perfect double helix in order to better understand the origin of stabilization. Melting temperatures were also measured with the complementary sequence embedded in a larger nucleic acid strand, a situation typically found with oligonucleotide probes. Variation of the oligonucleotide/oligospermine ratio was expected to highlight the relative contribution of ionic forces to nucleic acid hybridization in general and to polyamine binding to single stranded and double stranded nucleic acids in particular and hence provides rules for predicting the stability of any oligonucleotide–oligospermine duplex.

**Synthesis of the Cationic Oligonucleotides.** Stepwise coupling of nucleic bases and spermine residues was performed on an oligonucleotide synthesizer using the phosphoramidite chemistry. Ultramid protecting groups and standard coupling conditions were used for the nucleic bases dimethoxytrityl phosphoramidites. The fifth synthon was a dimethoxytritylspermine phosphoramidite derivative<sup>17</sup> (Figure 1) which was allowed to react using a twice-increased coupling time. Syntheses were performed on a 1 μmole scale. Cationic oligonucleotides were

(17) Voirin, E.; Behr, J. P.; Kotera, M. *Nature Protocols* **2007**, *2*, 1360–1367.

(18) Chen, C. P.; Zhang, L. R.; Peng, Y. F.; Wang, X. B.; Wang, S. Q.; Zhang, L. H. *Bioconjugate Chem.* **2003**, *14*, 532–8.

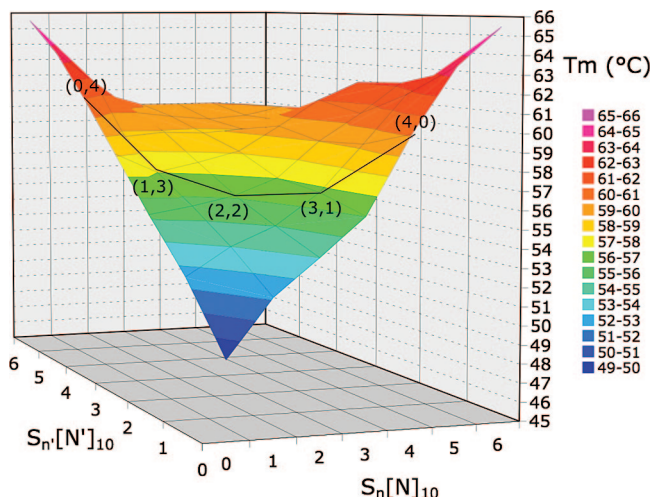


**Figure 2.** 3-D plot of melting temperatures ( $T_m$ ) of decamer duplexes  $S_n[N]_{10} \cdot S_{n'}[N']_{10}$  with up to  $n = n' = 6$  conjugated spermine residues. Measurements performed at  $3.5 \mu\text{M}$  duplex concentration in 150 mM NaCl, 10 mM HEPES, pH 7.4.

cut off the resin and fully deprotected at once, DMT-ON purified, and characterized by HPLC and MALDI-TOF (see Supporting Information). Oligonucleotide–oligospermine conjugates are conventionally written from the 5' to the 3' end, hence  $S_n[N]_m$  is a  $m$ -mer oligonucleotide of sequence NNN.. (or of complementary sequence N'N'N'..) 5'-conjugated with  $n$  spermine residues.

A decanucleotide sequence  $[N]_{10} = 5'\text{GCG ATG CCA C}$  originating from the green fluorescent protein gene was 5'-conjugated with 0, 1, 2, 3, 4, 5, 6, 8, 10, 15, and 20 spermine residues. Its complementary sequence  $[N']_{10}$  was either 5' or 3'-appended to 0, 1, 2, 3, 4, 5, and 6 spermine residues (Figure 1). Hairpin oligonucleotides having this sequence as the stem and either an oligospermine-containing loop  $[\text{GTG GCA TCG C}]S_6T_6[\text{GCG ATG CCA C}]$  and  $[N']_{10}S_6[N]_{10}$ , or a 5' conjugated oligospermine  $S_6[N']_{10}T_6[N]_{10}$  were synthesized as well (Figure 1). 3'-Shortened octanucleotides and hexanucleotides  $[N]_8$  and  $[N]_6$  from the same sequence were 5'-conjugated with 0, 1, and 2 spermine residues. An eicosanucleotide  $[N]_{20}$  of sequence TGG AAG ATG GAA CCG CTG GA originating from the *P. pyralis* firefly luciferase gene and the corresponding end codon-trimmed tetradecanucleotide  $[N]_{14}$  were 5'-conjugated with 0, 3, 4, 5 and 0, 2, 3, 4 spermine residues, respectively. Individual coupling yields were within the range of 92–98%, as measured by the released trityl cation.

**Ionic and Watson–Crick Contributions to Duplex Formation.** A large set of data had to be generated prior to attempting to derive general rules. The melting temperature  $T_m$  was therefore measured for all combinations of  $S_n[N]_{10} \cdot S_{n'}[N']_{10}$  duplexes, up to  $n = 6$ , where the oligospermine cationic charge is capable of neutralizing the 18 phosphate anions borne by the decanucleotide duplex. In effect, each tetraamine spermine residue being conjugated via a phosphate group (Figure 1) accounts for a global  $+4 - 1 = +3$  charge if the amines are fully protonated, hence  $S_6[N]_{10}^{+9}$ . Data corresponding to the  $T_m(n, n')$  matrix are shown in Table 1 and represented as a surface in Figure 2 (for experimental conditions, see Supporting Information).

As seen from the blue to red  $T_m$  gradient in Figure 2, the most prominent feature is that all spermine-containing duplexes ( $n, n' \neq 0$ ) are more stable than the natural one ( $n = n' = 0$ ;  $T_m$

**Table 1.** Melting Temperatures ( $T_m$ , °C) of  $S_n[N]_{10} \cdot S_{n'}[N']_{10}$  Duplexes in 150 mM NaCl

$n$ of $S_n[N]_{10}$	$n'$ of $S_{n'}[N']_{10}$						
	0	1	2	3	4	5	6
0	49.1	52.5	55.2	58.1	61.0	63.6	65.5
1	52.1	54.0	55.6	57.0	58.7	61.7	62.5
2	53.0	55.0	56.1	57.5	58.9	59.8	60.7
3	56.0	56.7	57.0	58.1	58.8	59.5	60.0
4	60.1	59.2	59.0	59.5	59.0	59.3	60.0
5	63.5	61.8	60.5	61.0	59.5	59.5	60.0
6	65.5	63.0	62.2	62.0	60.2	60.0	59.9

= 49 °C). This sounds obvious because interstrand phosphate anion repulsion is reduced, yet when  $n$  and  $n'$  are above 3, both oligos are formally cationic and could again repel each other. But instead of a decrease, a very broad plateau with average  $T_m = 59.7 \pm 0.7$  °C is observed. It can be rationalized by taking into account the striking structural and conformational differences between the anionic and cationic moieties of the duplex: the duplex conformation is a B-form helix, as assessed by the characteristic CD spectra (Supporting Information). This one-turn B-DNA double helix is rigid, with fixed intra- and interstrand phosphate distances, whereas the appended spermine residues are flexible and extended on average. Regarding relative sizes, molecular modeling shows that a fully extended protonated spermine residue spans up to five nucleotides. Because of a higher negative potential and the presence of ribose O(4'), pyrimidine O(2), and purine N(3) bidentate hydrogen bond-accepting atoms, spermine  $\text{NH}_2^+$  groups bind preferentially into the minor groove<sup>19</sup> and are capable of neutralizing closeby phosphates, thus releasing bound water and  $\text{Na}^+$  into the solution bulk.<sup>20,21</sup> To some extent, these conformational differences and electrostatic interactions hold also before hybridization<sup>22</sup> because single strands are conformationally poised for duplex formation.<sup>23</sup> Duplex stability is thus increasing with  $n$  and  $n'$  up to  $n = n' = 3$  because of decreasing interstrand phosphate anion repulsion. For  $n = n' = 3$ ,  $T_m = 58.1$  °C, each ampholyte strand is formally neutral, interstrand repulsion is lowest, and the  $S_3[N]_{10}^0 \cdot S_3[N']_{10}^0$  duplex stability is merely reflecting base pair formation. In agreement with this interpretation, a preliminary study<sup>24</sup> has shown that melting of the neutral/natural  $S_3[N]_{10}^0 \cdot [N']_{10}^{-9}$  duplex was salt-independent. Moreover, the calculated<sup>25</sup>  $T_m$  for the  $[N]_{10}^{-9} \cdot [N']_{10}^{-9}$  duplex of sequence GCG ATG CCA C at very high salt concentration, where ionic repulsion is shielded, is culminating at 58.4 °C. Onset of the plateau is thus corresponding to the Watson–Crick contribution to duplex stability. Further increasing the length of the spermine moieties beyond  $n = n' = 3$  does not decrease stability because, in contrast to interstrand phosphate groups which are held at fixed distances upon duplex formation, the flexible and extended spermine residues can avoid each other as schematically depicted in Figure 3a.

(19) Schmid, N.; Behr, J. P. *Biochemistry* **1991**, *30*, 4357–4361.

(20) Manning, G. S. *Q. Rev. Biophys.* **1978**, *11*, 179–246.

(21) Braunlin, W. H.; Strick, T. J.; Record, M. T., Jr. *Biopolymers* **1982**, *21*, 1301–1314.

(22) Mascotti, D. P.; Lohman, T. M. *Proc. Natl. Acad. Sci. U.S.A.* **1990**, *87*, 3142–3146.

(23) Vesnaver, G.; Breslauer, K. J. *Proc. Natl. Acad. Sci. U.S.A.* **1991**, *88*, 3569–3573.

(24) Pons, B.; Kotera, M.; Zuber, G.; Behr, J.-P. *ChemBioChem* **2006**, *7*, 1173–1176.

(25) OligoAnalyzer <http://eu.idtdna.com/analyzer/Applications/OligoAnalyzer/Default.aspx>.

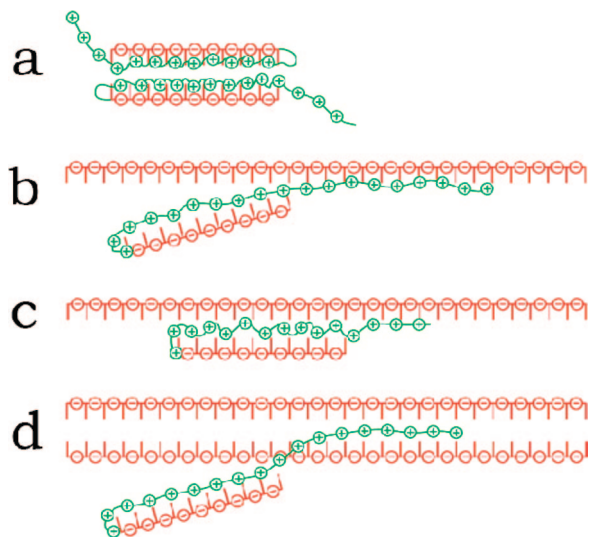


**Figure 3.** Illustration of various complex formation modes (see text).

The second interesting topographical feature of the  $(n, n')$   $T_m$  surface is the valley that runs through the middle of the  $(n, n')$  plane, from  $(0, 0)$  to  $(6, 6)$ . It is highlighted in Figure 2 by the  $(n + n' = 4)$  section perpendicular to the diagonal axis. This valley shows that, for a given total number  $(n + n')$  of spermine residues in the duplex, it is always preferable to have them all on one strand. This makes sense since it is corresponding to the most favorable/least unfavorable electrostatic situation toward duplex formation. Remarkably, the surface is quasi-symmetrical with respect to this axis, as judged by the small average difference between the 42 measured  $T_m(n, n')$  and  $T_m(n', n)$  values,  $\sum(T_m(n, n') - T_m(n', n))/21 = 0.09$  °C, and an rms deviation of 0.9 °C. Since the GCG ATG CCA C sequence has no symmetry with respect to sequence or AT/GC or Pu/Py distribution, this is an indirect confirmation of the earlier conclusion<sup>19,26</sup> that spermine has no marked sequence preference (unless long A,T-rich stretches are narrowing the minor groove).

As depicted in Figure 3a, long  $(n > 3)$  5'-spermine extensions can avoid each other in the duplex. However, a short 5'-conjugated spermine facing a 3'-conjugated one may in principle have a destabilizing effect, which should be favorable for DNA invasion<sup>7,27</sup> by  $S_n[N]_m \cdot [N']_m S_n$  duplexes. To test this hypothesis, we synthesized a series of 3'-conjugated  $[N']_{10} S_n$  oligonucleotides and measured their duplex melting temperatures with  $S_n[N]_{10}$ .  $T_m$ 's were generally found lower for the 3'/5' than for the 5'/5' modified duplexes (data not shown). However, the small magnitude of this effect (1–3 °C) shows that stability brought about by spermine is primarily due to single strand neutralization prior to hybridization, whether 5' or 3', and that neighboring spermines do not significantly hinder each other in the duplex.

Increasing the number of spermine residues up to six monotonically increased the stability of duplexes formed with the natural complementary strand, as seen along the  $n$  and  $n'$  axes in Figure 2, with no sign of saturation. In order to push electrostatic interactions to their asymptotic regime, we synthesized additional decamer oligonucleotides bearing 8, 10, 15, and 20 spermine residues and measured their duplex melting temperatures with  $S_{0-6}[N']_{10}$  (for individual values, see Table

3 of Supporting Information). Results shown in Figure 4 highlight again some interesting general features.

All duplexes where at least one strand is neutral have melting temperatures close to 60 °C, which is corresponding to the intrinsic stability of the Watson–Crick base pairing as discussed previously. This is true all along for the  $S_4[N']_{10}$  oligonucleotide whose  $T_m$  vs  $n$  curve stays nearly flat from  $n = 0$  to 20. This is also why all  $T_m$  curves intersect at a  $T_m = 59$ –60 °C for  $n = 3.5$ –4 (Figure 4). Finally, neutral or cationic  $S_{4-6}[N']_{10}$  oligonucleotides also have the  $T_m = 60$  °C above  $n = 4$  because excess cationic spermines can avoid each other.

The fact that the  $S_3[N']_{10}$  curve still shows a small repulsive ( $n < 3$ )/attractive ( $n > 4$ ) behavior and that the common intersection point lies at  $n = 3.5$ –4 rather than 3 is indication that not all amines are fully protonated at pH = 7.4 although the lowest  $pK_a$  of spermine itself is 8.4. Indeed, spermine oligomerization will result in a sequential decrease of individual amine  $pK_a$ s, but the oligonucleotide neighborhood and regularly spaced interspermine phosphodiester anions should counteract this effect. In order to force amine protonation, the melting of  $S_{1,2,4,6}[N]_{10} \cdot [N']_{10}$  duplexes was measured at pH = 6.4 instead of 7.4. A moderate 0.2–1.4 °C  $T_m$  increase was observed (data not shown) in agreement with the above explanation.

With respect to the  $T_m \sim 60$  °C horizontal line in Figure 4, all duplexes with lower  $T_m$  are composed of negatively charged single strands and all duplexes with a higher  $T_m$  have oppositely charged single strands. The highest  $T_m$ 's are observed with the natural  $[N']_{10}^{-9}$  strand which shows an asymptotic regime culminating at ca. 72 °C for  $n > 15$ . Such a rather slow-increasing regime may be a consequence of the fast-increasing distance between  $[N']_{10}$  and distal spermines of  $S_n[N]_{10}$  in the duplex. The actual position of the asymptote can be estimated to be ca. 75 °C from a previous  $T_m$  measurement of  $S_6[N]_{10}^{+9} \cdot [N']_{10}^{-9}$  in the absence of salt,<sup>24</sup> i.e., when electrostatic attraction is not shielded.

From the straight  $T_m$  vs  $S_n[N]_{10} \cdot [N']_{10}$  ( $n = 1$ –5) line, the average gain of stability for hybridization to a complementary natural decamer was estimated to be 2.9 °C/spermine in 150 mM salt. This ca. 1 °C increase per charge is to be compared with a similar increase for spermine linked to the N(2) of guanines in a 22-mer oligonucleotide,<sup>28</sup> and to a 2 °C per charge for octa<sup>12</sup> or nonanucleotide–peptide conjugates<sup>29</sup> in 100 mM salt. However,  $\Delta T_m$ /charge is quickly decreasing with increasing salt concentration<sup>24</sup> and with oligonucleotide length (see below), which makes comparisons between the above-mentioned compounds difficult.

**Oligonucleotide–Oligospermine Probes.** In practical situations, oligonucleotides are designed to hybridize to a target sequence borne by a much longer nucleic acid. We therefore measured  $T_m$  for  $S_n[N]_{10} \cdot [N']_{45}$  duplexes where the complementary sequence is in the middle of a 45-mer oligonucleotide (sequence in Supporting Information).  $T_m$  of the  $[N]_{10} \cdot [N']_{45}$  duplex ( $n = 0$  in Figure 5) was 1.6 °C lower than that of the  $[N]_{10} \cdot [N']_{10}$  duplex (49.1 °C, Figure 4), reflecting a larger repulsion between the two strands. To our surprise, the  $T_m$  was increasing more than twice faster with  $n$  than previously ( $\Delta T_m$ /spermine = 6.2 °C) and had reached its asymptote for  $n = 6$  (bold line in Figure 5). This robust increase may be due to the

(26) Hirschman, S. Z.; Leng, M.; Felsenfeld, G. *Biopolymers* **1967**, *5*, 227–233.

(27) Smulevitch, S. V.; Simmons, C. G.; Norton, J. C.; Wise, T. W.; Corey, D. R. *Nat. Biotechnol.* **1996**, *14*, 1700–1704.

(28) Potier, P.; Abdennaji, A.; Behr, J. P. *ChemBioChem* **2000**, *6*, 4188–4194.

(29) Wei, Z.; Tung, C. H.; Zhu, T.; Dickerhof, W. A.; Breslauer, K. J.; Georgopoulos, D. E.; Leibowitz, M. J.; Stein, S. *Nucleic Acids Res.* **1996**, *24*, 655–661.

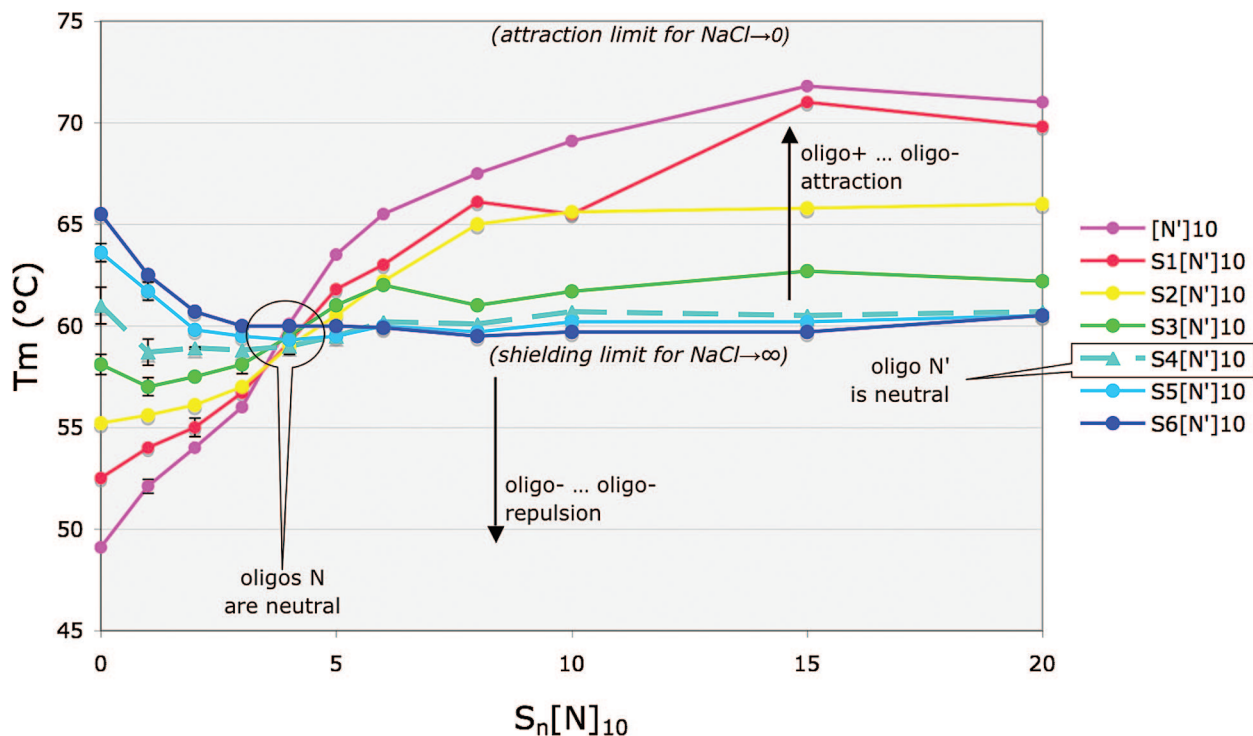


**Figure 4.** Plot of melting temperatures of duplexes  $S_n[N]_{10} \cdot S_n[N']_{10}$  vs number of spermines  $n$  up to 20. All duplexes with at least one neutral oligonucleotide–oligospermine strand have a  $T_m$  of ca. 60 °C. Experimental conditions as in Figure 2.

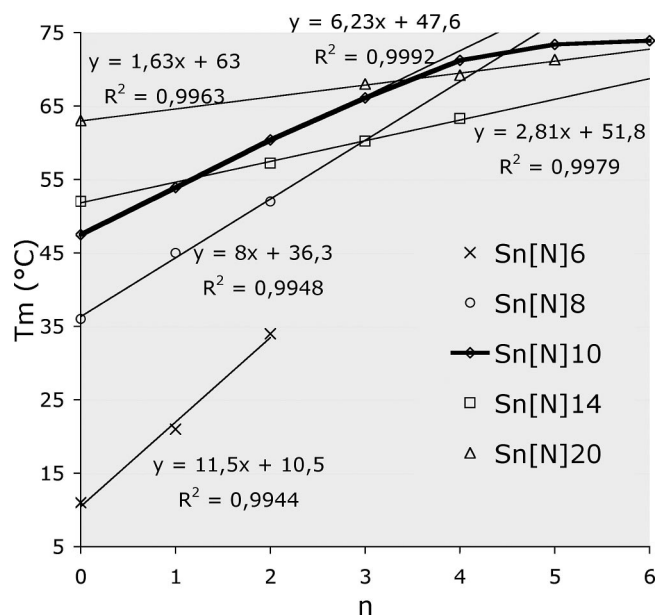


**Figure 5.**  $T_m$  is proportional to the number  $n$  of conjugated spermines. Melting temperatures of 6-, 8-, 10-, 14-, and 20-mer oligonucleotide probes bound to complementary sequences within 45–59-mer oligonucleotides were plotted vs the number  $n$  of conjugated spermines. The best-fit line equations are indicated. Experimental conditions as in Figure 2.

larger initial repulsion between the strands, hence a larger effect upon compensation by spermine. More precisely, decanucleotides are short and hence entirely subject to so-called “coulombic end effects” which limit electrostatic interactions even in their central portion, whereas the center of a 45-mer strand can be considered as a negatively charged infinite rod.<sup>30,31</sup> An attempt was made to confirm this explanation with  $S_n[N]_{10} \cdot [N']_{45}$  duplexes where the target sequence was at the 3' or 5'

end of the 45-mer. Self-hybridization of the 45-mers prevented accurate determination of melting temperatures, but  $T_m$ 's were indeed found ca. 3 °C lower for  $n = 5$  and 6 (data not shown).

The  $T_m$  increment per spermine was expected to vary with the oligonucleotide probe length rather than with its actual sequence (see above). We therefore measured the slopes of the  $T_m$  vs  $n$  lines before saturation for various oligonucleotide lengths. Hexa-, octa-, and deca-nucleotides were hybridized to a centrally located target within a 45-mer oligonucleotide. Because of their length, tetradeca- and eicosanucleotide targets had to be included into a longer 59-mer sequence (unnecessarily long targets would be reducing the relative magnitude of the hyperchromic melting shift). Data are shown in Figure 5 together with their best fit equations. The  $\Delta T_m$ /spermine slopes were abruptly decreasing as the oligonucleotide length was increasing. Yet were the slopes decreasing because of a decreasing relative impact of a spermine on an increasing number  $m$  of phosphates, irrespective of sequence, or on an increasing initial duplex stability ( $T_m$ )? To answer this question, we shifted the  $T_m$  of the decamer duplex by forming a hairpin loop. A  $T_6$  loop ( $[N']_{10}T_6[N]_{10}$ ) shifted  $T_m$  of the natural  $[N']_{10} \cdot [N]_{10}$  duplex from 49.1 to 69 °C. The  $S_6[N']_{10}T_6[N]_{10}$  duplex with spermines and loop on opposite ends showed a narrow melting at 82 °C, whereas  $S_6$  and  $S_6T_6$  loops gave extremely broad melting curves, presumably because of a large stability gradient along the duplexes. Conjugation of six spermines thus raised the  $T_m$  of the hairpin decamer duplex from 69 to 82 °C ( $\Delta T_m = 13$  °C) whereas the  $T_m$  of the simple decamer duplex had increased from 49.1 to 65.5 °C ( $\Delta T_m = 16.4$  °C, Figure 4). In conclusion, a 20 °C  $T_m$  shift resulted only in a 20% decrease of  $\Delta T_m$ /spermine (which altogether may be due to the hexamer loop),

(30) Zhang, W.; Ni, H.; Capp, M. W.; Anderson, C. F.; Lohman, T. M.; Record, M. T., Jr. *Biophys. J.* **1999**, *76*, 1008–1017.

(31) Shkel, I. A.; Ballin, J. D.; Record, M. T., Jr. *Biochemistry* **2006**, *45*, 8411–8426.



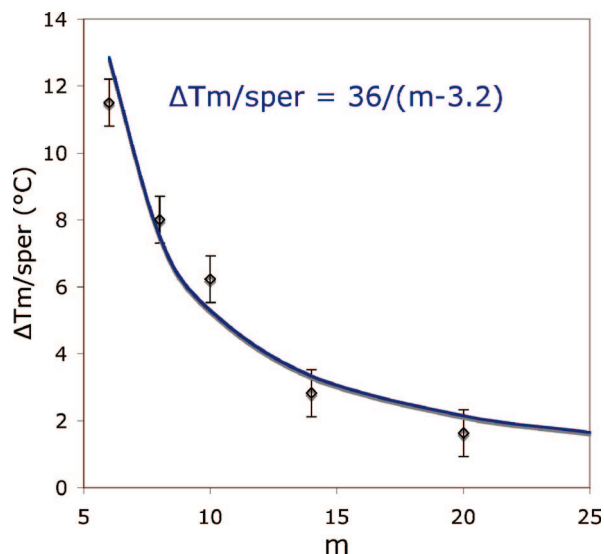


**Figure 6.** The  $T_m$  increase per conjugated spermine is only dependent on the length  $m$  of the oligonucleotide.

thus pointing to the influence of the number of phosphates rather than initial  $T_m$  on  $\Delta T_m/\text{sper}$ .

We therefore plotted the  $\Delta T_m/\text{spermine}$  increment as extracted from the slopes in Figure 5 vs the oligonucleotide length  $m$ . Data are shown in Figure 6 with estimated  $\pm 0.7$  °C error bars. The data appearance prompted us to fit them with an hyperbole. For large oligonucleotides, the per spermine contribution to the  $T_m$  should tend to be toward zero. Data were therefore fitted with a  $y = A/(x - B)$  equation. The best fit that was obtained for  $A = 36$  and  $B = 3.2$  is drawn in Figure 6. Fortuitously or not, the vertical asymptote ( $m = 3.2$ ) is matching the three base pair nucleus required for a zipper-driven double helix to form.<sup>32</sup>

## Conclusion

Following development of a convenient synthesis, we have been able to undertake the first extensive study of oligonucleotide–oligocation conjugates. For practical reasons, data interpretation remained intuitive rather than thermodynamic. Thanks to regularly spaced anions and cations, and to the nondirective nature of electrostatic forces, the essence of this study could be condensed into a simple mathematic relation for predicting the  $T_m$  of any oligonucleotide–oligospermine conjugate. The possibility of raising the melting temperature of short 8–12-mer oligonucleotide probes to 60–70 °C in a known and sequence-independent way is of prime importance for multiplex quantitative PCR. Temperature shifting is presently being performed

using locked nucleic acids (LNA), but with tedious corrections, including number and type of modified bases as well as nearest-neighbor effects, that take into account a  $T_m$  shift range per locked base of  $-0.6$  °C to  $+7.2$  °C.<sup>33</sup> It can also be performed as a single ca. 20 °C jump using a minor groove binder.<sup>2</sup> In comparison, spermine conjugation is raising the  $T_m$  of 8–12-mer oligonucleotides to PCR temperatures in a smooth (4 to 7 °C/spermine) and accurate way while preserving mismatch discrimination.<sup>24</sup>

In regards to the mechanism, data are in agreement with neutralization of phosphate anions by the conjugated oligocations in the single-stranded species, thus reducing repulsion between complementary strands upon duplex formation. Inter-strand phosphate repulsion in a natural duplex, even for a decamer in physiological salt concentration, is having a large negative impact ( $-15$  °C) on stability brought about by base-pair formation. Conversely, attraction between oppositely charged decamers is having an even larger impact ( $+20$  °C), this time reinforcing base-pair formation.

With larger target oligonucleotides, still more robust increases are observed, but the limiting  $T_m$  values remain the same. Initially, we hoped that extended oligocation tails would favor encounter between an overall cationic oligonucleotide and a natural oligonucleotide target prior to hybridization (as depicted in Figure 3b), and cations to increase stability of bound probes beyond neutralization of the formed duplex (Figure 3c). Unfortunately, data show no evidence for this to occur, at least not in 150 mM salt. Cationic tails may still be important in cases where the target is duplex DNA (Figure 3d), such as DNA invasion or triplex formation by oligonucleotide–oligospermines, because spermine is having higher affinity for double-stranded than for single-stranded DNA.<sup>34,35</sup> Work along these lines is in progress.

**Acknowledgment.** We thank the Région Alsace for fellowships to R.N. and B.P. We warmly thank Dr Patrick Wehrung for mass spectrometry data of the conjugates.

**Supporting Information Available:** Oligonucleotide–oligospermine sequences and syntheses; analytical HPLC and MALDI-TOF data; melting temperature measurements; individual  $T_m$  values; CD spectra. This material is available free of charge via the Internet at <http://pubs.acs.org>.

JA804727A

- (33) McTigue, P. M.; Peterson, R. J.; Kahn, J. D. *Biochemistry* **2004**, *43*, 5388–5405.  
 (34) Morgan, J. E.; Blankenship, J. W.; Matthews, H. R. *Arch. Biochem. Biophys.* **1986**, *246*, 225–232.  
 (35) Basu, H. S.; Schwietert, H. C.; Feuerstein, B. G.; Marton, L. J. *Biochem. J.* **1990**, *269*, 329–334.

(32) Porschke, D. *Mol. Biol. Biochem. Biophys.* **1977**, *24*, 191–218.